Neuropilin 1 signaling guides neural crest cells to coordinate pathway choice with cell specification

Quenten Schwarz, Charlotte Henrietta Maden, Joaquim M. Vieira, and Christiana Ruhrberg[1]

Institute of Ophthalmology, University College London, 11-43 Bath Street, London EC1V 9EL, United Kingdom

Edited by Alex L. Kolodkin, Johns Hopkins University School of Medicine, Baltimore, MD, and accepted by the Editorial Board February 18, 2009 (received for review November 12, 2008)

Neural crest cells (NCCs) are highly motile embryonic stem cells that delaminate from the neuroectoderm early during vertebrate embryogenesis and differentiate at defined target sites into various essential cell types. To reach their targets, NCCs follow 1 of 3 sequential pathways that correlate with NCC fate. The firstborn NCCs travel ventrally alongside intersomitic blood vessels to form sympathetic neuronal progenitors near the dorsal aorta, while the lastborn NCCs migrate superficially beneath the epidermis to give rise to melanocytes. Yet, most NCCs enter the somites to form the intermediate wave that gives rise to sympathetic and sensory neurons. Here we show that the repulsive guidance cue SEMA3A and its receptor neuropilin 1 (NRP1) are essential to direct the intermediate wave NCC precursors of peripheral neurons from a default pathway alongside intersomitic blood vessels into the anterior sclerotome. Thus, loss of function for either gene caused excessive intersomitic NCC migration, and this led to ectopic neuronal differentiation along both the anteroposterior and dorsoventral axes of the trunk. The choice of migratory pathway did not affect the specification of NCCs, as they retained their commitment to differentiate into sympathetic or sensory neurons, even when they migrated on an ectopic dorsolateral path that is normally taken by melanocyte precursors. We conclude that NRP1 signaling coordinates pathway choice with NCC fate and therefore confines neuronal differentiation to appropriate locations.

semaphorin | sensory neuron | sympathetic neuron | peripheral nervous system

Neural crest cells (NCCs) are embryonic stem cells that delaminate from the neuroectoderm early during vertebrate development and then disseminate through the body to differentiate at defined target sites into various cell types (1). In the trunk, they give rise to the melanocytes and all neurons and glia of the peripheral nervous system (PNS). To reach their targets, the trunk NCCs of higher vertebrates migrate along 1 of 3 sequential pathways, which correlate with NCC fate (2–5). The choice of migratory pathway is intimately linked to somitogenesis, the process in which mesodermal structures called somites are added to the elongating embryo in a rostrocaudal fashion. Thus, at the level of each newly formed somite, the firstborn NCCs travel ventrally alongside intersomitic blood vessels and form sympathetic neuronal progenitors near the dorsal aorta (early NCC wave), whereas the lastborn NCCs migrate superficially beneath the epidermis to form melanocytes in the skin (late NCC wave). Yet, most NCCs travel ventromedially into the anterior sclerotome of each somite (intermediate wave). These NCCs either traverse the sclerotome to give rise to sympathetic neurons at the dorsal aorta, or they stall within the somite to differentiate into sensory neurons. A fundamental, yet unanswered question therefore is how NCC migration is directed into the 3 temporally and spatially distinct pathways. Two other key questions are whether NCCs need to migrate through the sclerotome to receive instructive signals for acquisition of a sensory fate and how the choice of migratory pathway impacts on PNS segmentation. To answer these questions, we identified the molecular mechanism that controls the choice between the intersomitic and sclerotome routes and examined how the disruption of this mechanism impacts on gangliogenesis in the trunk. Here we show that a previously described ligand/receptor pair consisting of the repulsive guidance cue SEMA3A (6) and its transmembrane receptor neuropilin 1 (NRP1) (7, 8) plays a hitherto unidentified role in controlling trunk NCC migration. Thus, loss of SEMA3A/NRP1 signaling caused intermediate wave NCC precursors to migrate into the intersomitic furrow at the expense of the anterior sclerotome and thereby disrupted the rostrocaudal and dorsoventral patterning of the PNS ganglia in the trunk.

Results

Even though SEMA3A collapses chick NCCs in vitro (9), NRP1 was reported to be dispensable for trunk NCC patterning in the mouse (10). We therefore asked if SEMA3A and NRP1 control a previously unidentified mechanism in trunk NCC migration. Consistent with this idea, we found that their expression at 9.5 days post coitum (dpc) in the mouse correlated with a precisely controlled switch of NCC migration from the intersomitic to the sclerotome path (Fig. 1; see also Fig. S1). Thus, the earliest wave of NCCs expressed the neuroglial NCC marker p75 neurotrophin receptor (11), but not NRP1 (Fig. 1*A*). These NRP1-negative NCCs migrated in the intersomitic furrow alongside intersomitic blood vessels and along the boundary of the anterior and posterior sclerotome ("von Ebner's Fissure"), a structure that morphologically resembles the intersomitic furrow (12) (Fig. 1*A*). In contrast, most NCCs in the intermediate wave coexpressed NRP1 and p75, both when they gathered in the migration staging area (MSA) above the somites (Fig. 1*B*) and when they entered the anterior sclerotome (Fig. 1*C*). Consistent with previous observations in cultured mouse embryos (13), we identified p75-positive NCCs between the dermomyotome and epidermis at this stage. However, these dorsolateral NCCs were rare relative to the number of NCCs in the sclerotome (Fig. 1 *D* and *E*). NRP1 was also expressed at low levels in somitic mesenchyme cells at this stage (Fig. 1 *A* and *C*; Fig. 2 *C* and *D*). In transverse sections, these mesenchymal cells could be distinguished from NCCs by lack of expression of *Sox10*, which encodes a transcription factor essential for NCC differentiation (14) (compare Fig. 2 *B* with *D*).

The *Sema3a* gene was expressed in a reciprocal pattern to NRP1 (Figs. 1 and 2). Thus, *Sema3a* was not expressed in the anterior sclerotome, where p75-positive NCCs migrated (Fig. 1*D*). Instead, *Sema3a* was prominent in the adjacent dermomyotome, firstly in an anterior stripe that bordered the preceding

Author contributions: Q.S. and C.R. designed research; Q.S., C.H.M., and J.M.V. performed research; Q.S. and C.R. analyzed data; and C.R. wrote the paper.

The authors declare no conflict of interest.

This article is a PNAS Direct Submission. A.L.K. is a guest editor invited by the Editorial Board.

Freely available online through the PNAS open access option.

[1]To whom correspondence should be addressed. E-mail: c.ruhrberg@ucl.ac.uk.

This article contains supporting information online at www.pnas.org/cgi/content/full/0811521106/DCSupplemental.

Fig. 1. *Nrp1* and *Sema3a* expression patterns during trunk NCC migration. (A–E) Longitudinal sections through a 9.5 dpc (25-somite) mouse embryo; only one-half of the section is shown; the neural tube is at the top of each panel; somites are counted backwards from the most recent pair formed. (A–C) Double labeling for the NCC marker p75 (green) and NRP1 (red). Early wave NCCs appeared to migrate alongside intersomitic blood vessels (isv) and expressed p75, but not NRP1 (arrow in *A*). In addition, some early NCCs migrated along the boundary between anterior and posterior sclerotome (curved arrow). (*B*) NCCs in the nonsegmented migration staging area (MSA) in the dorsal rostral trunk co-expressed p75 and NRP1 (yellow). (*C*) A section taken at the same rostral level, but further ventrally through the somites, showed that NCCs in the anterior sclerotome (arrowheads) co-expressed p75 and NRP1 (yellow). (*A* and *C*) Mesenchymal cells (wavy arrows) and neural progenitors in the neural tube also expressed NRP1, but at lower levels. (*D* and *E*) Triple labeling for *Sema3a* (blue), p75 (NCCs, green), and endomucin (blood vessels, red). (*D*) *Sema3a* was expressed in the posterior sclerotome and the dermomyotome, with highest levels in the anterior and posterior part of the dermomyotome, adjacent to the neighboring intersomitic furrows (clear arrow and arrowhead, respectively). The dimensions of the dermomyotome versus sclerotome and the anterior (a) versus posterior (p) sclerotome are indicated with brackets. (*E*) In wild-types, most intermediate wave NCCs migrated through the avascular anterior sclerotome (arrowhead), and only a few NCCs migrated alongside intersomitic vessels (arrow) or around the dermomyotome (open arrowhead). (*F*) Schematic representation of NRP1 and SEMA3A expression during trunk NCC migration in the 9.5 dpc mouse embryo. The firstborn trunk NCCs do not express NRP1 (green) and migrate through the intersomitic furrow or along the anteroposterior boundary within the sclerotome. Most NCCs in the intermediate wave are NRP1-positive (yellow) and migrate through the anterior sclerotome; they settle in the sclerotome or travel ventrally to meet NCCs from the early wave at the dorsal aorta; there, NCCs move rostrocaudally along the dorsal aorta to form the sympathetic anlagen. Abbreviations: da, dorsal aorta; dm, dermomyotome; isf, intersomitic furrow; isv, intersomitic vessel; psv, perisomitic vessel; pvp, perineural vascular plexus; sa, sympathetic anlage; scl, sclerotome. (Scale bars: *A*–*C*, 50 μm; *D* and *E*, 100 μm.)

intersomitic furrow and secondly in a domain that extended from the posterior dermomyotome into the posterior sclerotome (Fig. 1*D*, clear arrow and arrowhead, respectively). Wholemount analysis confirmed that *Sema3a* was expressed in metameric pairs of stripes and further revealed that both stripes extended along the dorsoventral axis of each somite (Fig. 2 *E* and *F*). In addition, wholemount in situ hybridization complemented the analysis of expression patterns in sections, as it provided an overview of NCC migratory pathways relative to *Nrp1* and *Sema3a* expression domains (compare Fig. 2 *A* with *C* and *E*).

Because early wave, but not intermediate wave NCCs were previously proposed to follow blood vessels in the intersomitic

Fig. 2. *Nrp1* and *Sema3a* expression during trunk NCC migration. Wholemount in situ hybridization (ISH) for *Sox10* (*A* and *B*), *Nrp1* (*C* and *D*), and *Sema3a* (*E* and *F*) of 9.25 dpc (20–21 somite stage) mouse embryos. (*A* and *C*) Trunk NCCs express *Sox10* and *Nrp1* and migrate into the anterior sclerotome (black arrowheads), while the posterior sclerotome remains NCC-free (brackets); the arrows indicate the region where the sympathetic chain begins to assemble. (*E*) *Sema3a* was expressed in pairs of vertical stripes, 1 in the anterior (empty arrow) and 1 in the posterior somite half (empty arrowhead). (*B*, *D*, and *F*) Transverse sections through the wholemount samples shown in *A*, *C*, and *E* at the level of the anterior somite suggested that *Sox10* (*B*) and *Nrp1* (*D*) were co-expressed in NCC in the migration staging area (MSA), within the sclerotome (black arrowheads) and in NCC clusters (black arrows) adjacent to the dorsal aorta (da). *Nrp1* expression in *Sox10*-negative mesenchymal cells (wavy arrow; compare *B* with *D*). (*F*) *Sema3a* expression in the forelimb (fl) and the dermomyotome (dm). (Scale bars: *A*, *C*, and *E*, 250 μm; *B*, *D*, and *F*, 100 μm.)

furrow (2, 3), we compared the position of NCCs to that of blood vessels by double immunolabeling for p75 and the vascular endothelial marker endomucin (15). This analysis confirmed that only few NCCs normally traveled alongside blood vessels in the intersomitic furrow, but that the majority of NCCs instead entered the largely avascular anterior sclerotome at 9.5 dpc (Fig. 1*E*, arrow and arrowhead, respectively).

Since our expression analysis was consistent with a model in which SEMA3A prevents NRP1-expressing trunk NCCs from migrating into the intersomitic furrow to promote NCC entry into the anterior sclerotome (Fig. 1*F*), we next asked if this ligand/receptor pair was essential to control trunk NCC migration. Using wholemount in situ hybridization for *Sox10* to analyze mouse mutants lacking *Nrp1* (16), we identified 2 types of NCC defects in 8/8 cases (Fig. 3). Firstly, NCCs from the intermediate wave adopted a migratory pattern that is normally seen only in the minor early wave, with rerouting of most NCCs into the intersomitic furrow at the expense of the sclerotome (compare Fig. 3 *A* with *B* and *D* with *E*). Secondly, a few NCCs invaded the posterior sclerotome, which is normally NCC-free (clear arrowheads in Fig. 3*E*). However, the phenotype of posterior sclerotome invasion was less obvious than the excessive intersomitic invasion, because only few NCCs entered the sclerotome in the mutants (compare white arrowhead in Fig. 3 *D* with *E*; see also Fig. 4).

NRP1 is not only expressed in NCCs, but also in vascular endothelial cells and somitic mesenchyme (Figs. 1 and 2). We therefore asked if NRP1 was required cell-autonomously by trunk NCCs to control their behavior. To address this question, we ablated NRP1 specifically in NCCs using a conditional *Nrp1*-null allele (17) and CRE recombinase under the control of the *Wnt1*-promoter (18). We found that the NCC-specific *Nrp1*-null mutants phenocopied the defect of full *Nrp1*-null mutants, supporting the idea that NRP1 is expressed by NCCs to control their migration (compare Fig. 3 *B* with *C* and *E* with F; 4/4 cases). Transverse sections through the intersomitic furrow of embryos lacking NRP1 in NCCs further demonstrated that ectopic cells in the intersomitic furrow segregated into a dorsolateral and ventromedial stream (Fig. 3*H*, black arrow and double arrowhead, respectively). 5/5 embryos carrying a mutation that reduces semaphorin-binding to NRP1 (17) and 10/10 embryos with a

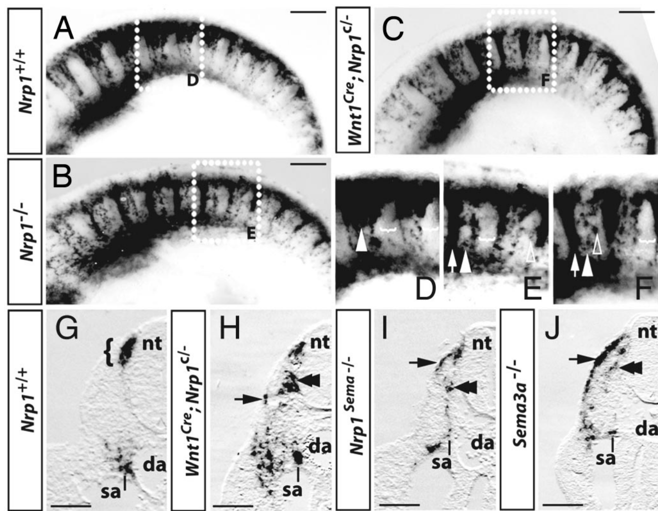

Fig. 3. SEMA3A/NRP1 signaling promotes NCC migration into the sclerotome. (*A–F*) In situ hybridization (ISH) for *Sox10* at 9.5 dpc (22–25 somite stage); (*D–F*) are higher magnifications of the boxed areas in (*A–C*). NCCs preferentially migrated into the anterior sclerotome in wild-types (*A*), but into the intersomitic furrows in full *Nrp1*-null (*B*) or NCC-specific *Nrp1*-null mutants (*C*); as an example, 1 NCC stream in the anterior sclerotome is indicated with an arrowhead and 1 of the intersomitic streams with an arrow in (*D–F*). Whereas wild-type NCCs avoided the posterior sclerotome (indicated with brackets in *D*), mutant NCCs occasionally invaded the posterior sclerotome (clear arrowheads in *E* and *F*). (*G–J*) Transverse sections through the intersomitic furrow of a wild-type (*G*), NCC-specific *Nrp1*-null mutant (*H*), and mutants deficient in semaphorin signaling through NRP1 (*I*) or in SEMA3A (*J*); half of each section is shown. At the level of the intersomitic furrow, wild-type NCCs were only seen in the migration staging area (bracket) adjacent to the dorsal neural tube and in the sympathetic anlagen (sa); in contrast, many mutant NCCs migrated into the intersomitic furrow, where they segregated into a ventromedial (double arrowheads) and dorsolateral (arrow) stream. Consequently, NCCs were seen scattered over a wide area near the dorsal aorta. Abbreviations: da, dorsal aorta; nt, neural tube; sa, sympathetic anlage. (Scale bars, 250 μm.)

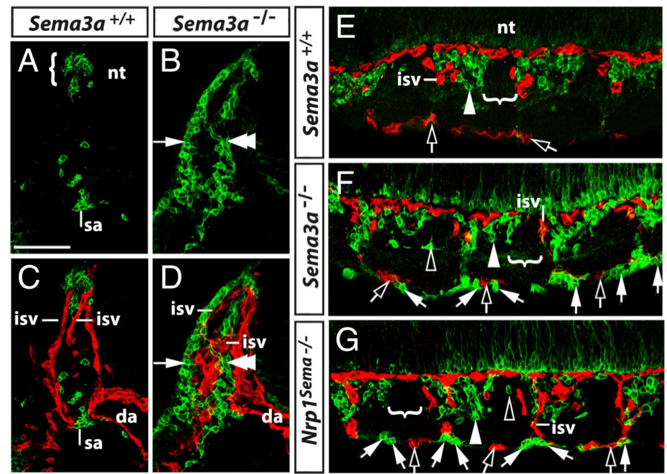

Fig. 4. Relationship of ectopic NCCs to blood vessels. Transverse (*A–D*) and longitudinal sections (*E–G*) stained for p75 (green) and endomucin (red) illustrate the relationship of NCCs to blood vessels at 9.5 dpc. (*A* and *B*) At the level of the intersomitic furrow, NCCs in wild-types accumulated in the MSA (bracket in *A*), whereas NCCs in *Sema3a*-null mutants formed a ventromedial (double arrowhead) and dorsolateral (arrow) stream that followed the course of intersomitic blood vessels (*C* and *D*). (*E*) Longitudinal sections demonstrated that most NCCs normally migrated into the anterior sclerotome (white arrowhead), but not into the posterior sclerotome (indicated with a bracket). (*F* and *G*) In *Sema3a*- and $Nrp1^{Sema}$-null mutants, only few NCCs entered the anterior sclerotome (white arrowhead), while most NCCs (white arrows) migrated alongside intersomitic and perisomitic vessels (clear arrows). In addition, ectopic NCCs were occasionally seen in the posterior sclerotome of mutants (clear arrowheads). Abbreviations: da, dorsal aorta; isv, intersomitic vessel; nt, neural tube; sa, sympathetic anlage. (Scale bar, 100 μm.)

Sema3a-null mutation (19) had a similar phenotype, with excessive NCC invasion of the intersomitic furrow in the form of dorsolateral and ventromedial streams and a few NCCs in the posterior sclerotome (Fig. 3 *I* and *J*; Fig. 4 *B* and *F*). SEMA3A/NRP1 signaling is therefore required to correctly pattern NCC migration along both the dorsoventral and anteroposterior axes of the embryo.

Given the prominent NCC defect of mutants deficient in SEMA3A/NRP1 signaling, we next asked why an earlier report erroneously concluded that NCC migration in *Nrp1*-null mice was normal and that NRP1 was essential only to pattern the neuronal progeny of sympathetic NCCs (10). We noted that this previous work relied on a marker that labels blood vessels in addition to NCCs, the 4E9R antibody (20). We therefore addressed if mutant NCCs migrated in close proximity to blood vessels, as this would make them difficult to visualize with a dual specificity reagent such as 4E9R. Consistent with this idea, double labeling of *Sema3a*-null mutants and *Nrp1*-mutants defective in semaphorin signaling with p75 and endomucin confirmed that ectopic NCCs followed the trajectory of blood vessels (Fig. 4; 7/7 cases). Thus, ectopic NCCs first migrated alongside intersomitic vessels (Fig. 4 *B* and *D*) and, after emerging from the intersomitic furrow, continued their migration by spreading rostrally and caudally around the somites in close proximity to perisomitic vessels (Fig. 4 *F* and *G*). Taken together, our observations establish that NRP1 is required cell autonomously in trunk NCCs as a receptor for SEMA3A to divert migrating NCCs from a path alongside blood vessels in the intersomitic and perisomitic space onto a path through the anterior sclerotome.

Because the NCC precursors of peripheral neurons are diverted from the usual sclerotome path in *Sema3a*- and *Nrp1*-null mutants, we next investigated the impact of these mutations on sensory and sympathetic gangliogenesis. We first used *Sox10* as a marker to follow the fate of ectopic NCCs, as it is not only present in the glial progeny of NCCs, but is also expressed transiently in neurogenic NCCs to initiate a transcriptional program for neuronal differentiation (21). At 9.75 dpc, when NCCs begin to condense into sensory ganglia (Fig. 5*A*), *Nrp1*-null mutants contained ectopic clusters of *Sox10*-positive cells at the level of the intersomitic furrow and above the somite (Figs. 5*B*, arrows). Transverse sections at 10.5 dpc demonstrated that *Nrp1*-null mutants assembled *Sox10*-positive anlagen for sensory and sympathetic ganglia, but that they were usually smaller than those of wild-type littermates and not present at all axial levels (compare Fig. 5 *C* with *D* and *E*). Moreover, we observed small clusters of ectopic *Sox10*-positive cells in dorsolateral positions, usually near small caliber blood vessels (insets in Fig. 5 *D* and *E*).

We next examined if the ectopic *Sox10*-positive NCC derivatives in *Nrp1*-null mutants were capable of differentiating into neurons with the Tuj1 antibody, which recognizes neuronal microtubules (22). We observed Tuj1-positive ectopic cell clusters in both dorsal and ventral positions in 3/3 cases (Fig. 5 *F* and *G*; compare top insets in Fig. 5 *D* and *G*). The ectopic clusters ventral to the neural tube co-expressed the sympathetic neuron marker tyrosine hydroxylase (TH) (23), with neuronal microtubules (Fig. 5 *G*, *J*, and *K*), indicating that they were differentiating into sympathetic neurons. The position of ectopic sympathetic neurons in the ventral trunk between the dorsal aorta and the limb correlated with the expression pattern of 2 secreted proteins that promote sympathetic differentiation, BMP4 and BMP7 (24). In contrast, the Tuj1-positive ectopic clusters in

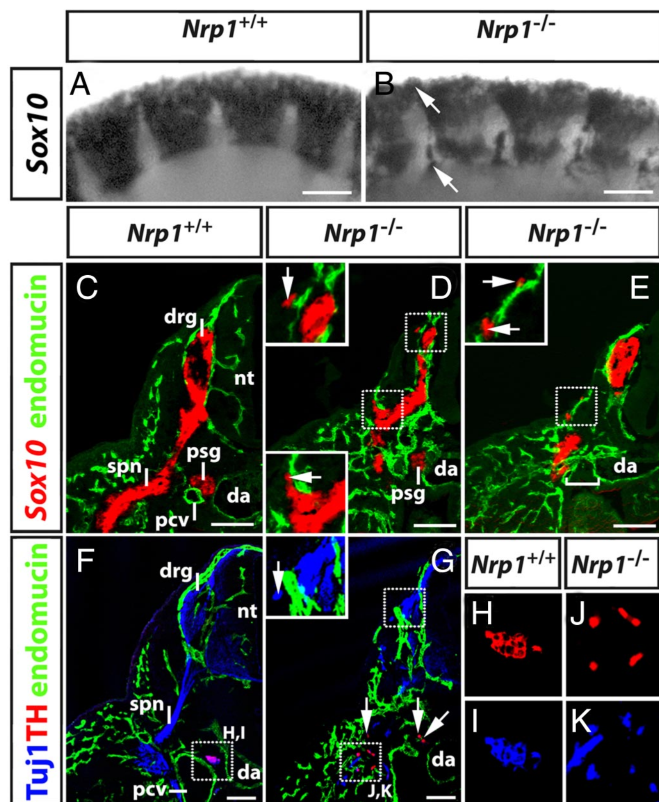

Fig. 5. Ectopic NCC migration impacts on PNS organization. (*A* and *B*) Wholemount in situ hybridization of 9.75 dpc wild-type and *Nrp1*-null embryos for *Sox10* revealed ectopic NCC near the dorsal neural tube and in the intersomitic furrows (arrows). (*C*–*E*) Transverse sections of 10.5 dpc wild-type and *Nrp1*-null embryos labeled for *Sox10* (red) and endomucin (green); half of each section is shown. (C) In wild-types, primary sympathetic ganglia (psg) formed between the dorsal aorta (da) and the posterior cardinal veins (pcv), while dorsal root ganglia (drg) form adjacent to the neural tube (nt) and extended 1 spinal nerve each (spn). (*D* and *E*) In mutants, dorsal root ganglia and primary sympathetic ganglia formed, but they were smaller than normal; at some axial levels, the sympathetic ganglia were missing (square bracket in *E*). The insets in *D* and *E* are higher magnifications of the squared areas and illustrate the proximity of ectopic cell clusters to superficial blood vessels. (*F* and *G*) Transverse sections of 10.5 dpc wild-type and *Nrp1*-null embryos labeled for neuronal microtubules (Tuj1; blue), endomucin (green), and the sympathetic marker tyrosine hydroxylase (TH; red). The inset in *G* is a higher magnification of the squared area and illustrates the presence of ectopic neuronal microtubule-positive, TH-negative neurons adjacent to the dorsal root ganglia. In mutants, TH-positive neuronal progenitors were scattered distally to the dorsal aorta. Ventral regions marked with squares in *F* and *G* are shown as separate color channels at higher magnification in *H* and *I* and *J* and *K*, respectively. (Scale bars, 100 μm.)

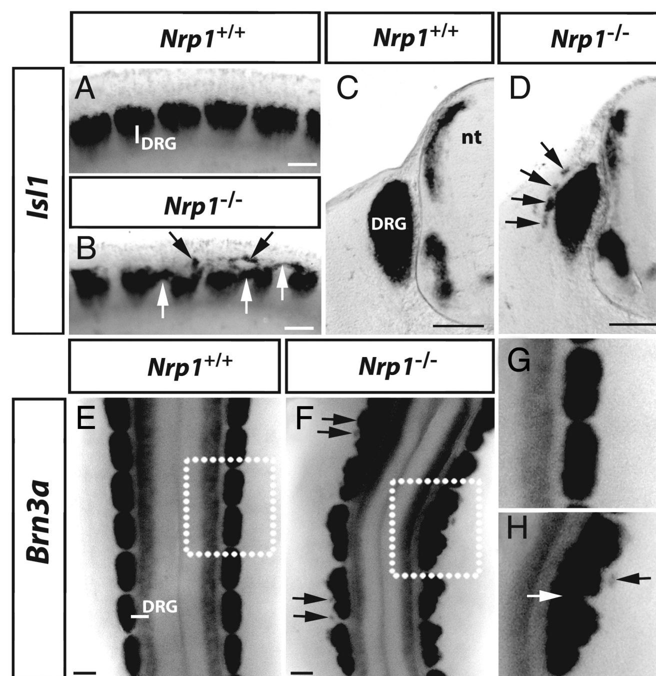

Fig. 6. Ectopic NCC migration perturbs DRG segmentation. (*A* and *B*) Lateral wholemount view and transverse sections (*C* and *D*) of 11.5 dpc wild-types and *Nrp1*-null mutants labeled with the sensory marker *Isl1*. (*E* and *F*) Dorsal wholemount view of 11.5 dpc wild-types and *Nrp1*-null mutants labeled with the sensory marker *Brn3a*; higher magnifications of the boxed areas in *E* and *F* are shown in *G* and *H*. Black and white arrows indicate ectopic neuron clusters in dorsolateral positions and between neighboring DRGs, respectively; note that the merging of neighboring DRGs is accompanied by abnormal curving of the neural tube in *F*. (Scale bars, 100 μm.)

dorsolateral locations did not express TH; instead, they expressed the sensory markers *Isl1* (25) and *Brn3a* (26), confirming that they contained sensory neurons (arrows in Fig. 6 *B*,*D*, *F*, and *H*, respectively; 4/5 and 4/4 cases, respectively). The identification of ectopic sensory neurons near the neural tube, but not in ventral positions was consistent with the observation that the neural tube releases factors essential for sensory neuron differentiation and survival (27). Taken together, our observations demonstrate that ectopic NCCs were able to fulfil their developmental potential, as they differentiated into sensory and sympathetic neurons depending on their dorsoventral position in the developing embryo.

Discussion

Trunk NCCs giving rise to neurons or glia usually migrate along a ventromedial path, with a minor first wave traveling through the intersomitic boundary and a second major wave migrating through the anterior sclerotome. We demonstrate here that the switch from the intersomitic to the sclerotome path is a prerequisite for the proper pattering of the PNS and that it is controlled by SEMA3A/NRP1 signaling. Firstly, *Sema3a* and *Nrp1* are expressed in a complementary fashion during trunk NCC migration: *Sema3a* in the posterior sclerotome and the entire dermomyotome, and *Nrp1* in NCCs that migrate through the sclerotome (Figs. 1 and 2). Secondly, loss of SEMA3A or NRP1 impairs the switch of NCC migration from the intersomitic to the sclerotome path and additionally causes splitting of the intersomitic stream into a ventral and dorsal component (Figs. 3 and 4). The finding that SEMA3A/NRP1 signaling controls trunk NCC migration in the mouse agrees with earlier in vitro work, which demonstrated that explanted chick NCCs collapse in response to SEMA3A (9). However, others suggested that NCC migration in *Nrp1*-null mice is normal and that NRP1 is essential only to pattern the neuronal progeny of sympathetic NCCs (10). This idea was derived from studies using the 4E9R antibody, which labels blood vessels in addition to NCCs (20). Because ectopic NCCs migrate in close association with blood vessels (Figs. 3 and 4), we conclude that this marker was unsuitable to analyze *Nrp1*-null mutants.

Pathway sharing of early NCCs and blood vessels likely promotes the recruitment of NCCs to the dorsal aorta to seed the sympathetic primordia. However, the precise role of blood vessels in guiding NCCs will have to await the identification of genetic mouse models that disrupt vascular growth in the intersomitic boundaries without perturbing the general blood supply essential for embryogenesis. Presently, there are 2 alternative explanations why NCCs preferentially travel on ectopic vascular pathways in the absence of inhibitory guidance signals

provided by SEMA3A/NRP1. On the one hand, blood vessels assemble an extracellular matrix rich in fibronectin (28), an effective substrate for NCC migration (29). Alternatively, NCCs and blood vessels may share a similar preference for matrix molecules and therefore invade similar regions independently of each other. In support of the latter hypothesis, early wave NCCs do not migrate exclusively alongside blood vessels in the intersomitic furrow, but also track the boundary between the anterior and posterior sclerotome, just before blood vessels invade this space (Fig. 1*A*).

Even though early sympathetic NCCs chose an intersomitic pathway to reach the dorsal aorta, most NCCs in higher vertebrates travel in the intermediate wave through the somites, giving rise to sympathetic or sensory neurons in appropriate place (Figs. 1–6). It was originally thought that the selective migration of NCCs through the anterior rather than posterior sclerotome of the somite was essential for the alignment of sensory neurons with spinal nerves and therefore PNS segmentation. However, losing the anteroposterior polarity of NCC migration within the somites by ablating SEMA3F/NRP2 signaling does not disrupt PNS segmentation (30). Our finding that SEMA3A/NRP1 signaling maintains a NCC-free space in the intersomitic furrows at the time of gangliogenesis (Fig. 3) finally explains why abolishing the selective migration of NCCs through the anterior sclerotome does not prevent PNS segmentation. Contrary to all previous expectations, the SEMA3A/NRP1-mediated switch of NCC migration from the intersomitic to the sclerotome pathway is therefore of greater importance for the segmentation of PNS neurons than the decision of NCCs to migrate through the anterior versus posterior sclerotome. Because SEMA3A/NRP1 signaling also confines NCC migration to the correct dorsoventral plane (Fig. 3), SEMA3F/NRP2 signaling is equally dispensable for the positioning of dorsal root and sympathetic ganglia along the dorsoventral axis (30, 31). Together, these data suggest that SEMA3A/NRP1 signaling is both required and sufficient to maintain NCCs on a segmental and ventromedial path (Fig. 7 *A* and *B*).

The switch in NCC migration from the ventromedial to the dorsolateral path correlates with a change in developmental destiny and can be followed with specific markers. For example, ventromedially migrating NCCs express p75 and have a neuroglial fate, whereas cells on the dorsolateral path express TRP2 and yield melanocytes (32, 33). Thus, it has been hypothesized that prespecification before or just after their emigration from the neural tube allows different NCC populations to enter distinct paths (34). Our study provides physiological evidence for the idea that p75/NRP1 co-expressing NCCs are specified toward a neuroglial fate and that this fate is not altered even if these cells lose their normal guidance factors and adopt a pathway that is normally taken only by the NCC precursors of melanocytes. NCCs therefore do not need to migrate through the sclerotome to receive instructive signals for the acquisition of a sensory or sympathetic fate (Figs. 5 and 6). Rather, NCC specification normally correlates with the choice of migratory pathway, because most neuroglial NCCs express NRP1 to enforce migration through the sclerotome (Fig. 7 *A* and *B*). NRP1 signaling therefore places trunk NCCs into appropriate positions along both the anteroposterior and dorsoventral axes to ensure the formation of a properly positioned PNS (Fig. 7 *C* and *D*). Taken together with our recent finding that SEMA3A/NRP1 also guides cranial NCC to organize placodal neurons (35), we conclude that SEMA3A/NRP1 signaling plays a fundamental and central role in organizing the PNS from the moment of its conception.

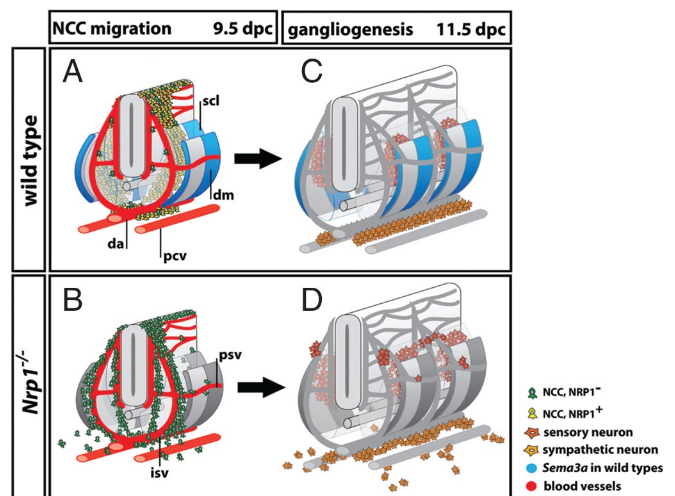

Fig. 7. Working model: SEMA3A and NRP1 control trunk NCC migration to organize PNS neurons. (*A* and *B*) NCC migration pathways at 9.5 dpc. (*A*) In wild-types, only a few intermediate wave NCCs are NRP1-negative (green) and travel alongside intersomitic and perisomitic vessels (red). Rather, most NCCs are NRP1-positive (yellow) and are channeled into the anterior sclerotome by repulsive SEMA3A signals. Accordingly, *Sema3A* (blue) is expressed in 2 domains, a narrow stripe in the dermomyotome adjacent to the preceding intersomitic furrow, and a broader domain in the posterior dermomyotome that extends into the posterior sclerotome. (*B*) In the absence of NRP1 signaling, intermediate wave NCCs are blind to SEMA3A (now shown in gray) and preferentially migrate alongside intersomitic blood vessels (red), similar to early wave NCCs. (*C* and *D*) Peripheral neuron position in wild-types and *Nrp1*-null mutants at 11.5 dpc reflects the migratory patterns of their NCC precursors. (*C*) In wild-types, sensory neurons condense into segmentally arranged dorsal root ganglia in the anterior sclerotome of the somites, while sympathetic neurons form paired, but nonsegmented primary sympathetic cords next to the dorsal aorta. (*D*) In the absence of SEMA3A/NRP1 signaling, sensory and sympathetic neurons differentiate in ectopic positions corresponding to the earlier position of their NCC precursors. Consequently, both the segmentation of the sensory system and the assembly of the sympathetic cords are disrupted. Abbreviations: da, dorsal aorta; dm, dermomyotome; isv, intersomitic vessel; psv, perisomitic vessel; pcv, posterior cardinal vein; scl, sclerotome.

Methods

Animals. To obtain mouse embryos of defined gestational ages, mice were mated in the evening, and the morning of vaginal plug formation was counted as 0.5 dpc. Somite numbers were used to stage-match embryos. Mice carrying a *Sema3a*- or *Nrp1*-null allele or a mutation that disrupts semaphorin-signaling through NRP1 have been described (16, 17, 19). Conditional null mutants for *Nrp1* (17) were mated to mice expressing CRE recombinase under the control of the NCC-specific *Wnt1* promoter (18) on a *Nrp1*+/− background. Mouse husbandry was performed in accordance with UK Home Office and institutional guidelines. Genotyping protocols can be supplied on request.

In Situ Hybridization and Immunolabeling. In situ hybridization was performed according to a previously published method (36) with digoxigenin-labeled riboprobes transcribed from cDNA-containing plasmids (15, 35). Immunolabeling was performed as described (15) using the following primary antibodies: For NCCs, rabbit anti-p75 (gift of K. Deinhardt and G. Schiavo, Cancer Research UK, London); for blood vessels, rat anti-endomucin (Santa Cruz Biotechnology); for neurons, mouse anti-neuron-specific class beta III tubulin (Tuj1; Covance); for sympathetic neurons, rabbit anti-tyrosine hydroxylase (Chemicon). For images of samples that had been fluorescently immunolabeled after in situ hybridization, the bright field image was inverted, pseudocolored, and merged with the fluorescent image using Adobe Photoshop (Adobe Systems).

ACKNOWLEDGMENTS. We thank Hajime Fujisawa, Masahiko Taniguchi, Andrew McMahon, Masahi Yanagisawa, David D. Ginty, and Alex L. Kolodkin for mouse strains. We thank the staff of the Biological Resources Unit for help with mouse husbandry. We are grateful to Matthew Golding for thoughtful comments on the manuscript. C.R. and coworkers are funded by the Medical Research Council, UK.

1. Le Douarin NM, Kalcheim C (1999) *The Neural Crest* (Cambridge University Press, New York) 2nd Ed.
2. Loring JF, Erickson CA (1987) Neural crest cell migratory pathways in the trunk of the chick embryo. *Dev Biol* 121:220–236.
3. Erickson CA (1985) Control of neural crest cell dispersion in the trunk of the avian embryo. *Dev Biol* 111:138–157.
4. Erickson CA, Duong TD, Tosney KW (1992) Descriptive and experimental analysis of the dispersion of neural crest cells along the dorsolateral path and their entry into ectoderm in the chick embryo. *Dev Biol* 151:251–272.
5. Thiery JP, Duband JL, Delouvee A (1982) Pathways and mechanisms of avian trunk neural crest cell migration and localization. *Dev Biol* 93:324–343.
6. Luo Y, Raible D, Raper JA (1993) Collapsin: A protein in brain that induces the collapse and paralysis of neuronal growth cones. *Cell* 75:217–227.
7. Kolodkin AL, et al. (1997) Neuropilin is a semaphorin III receptor. *Cell* 90:753–762.
8. He Z, Tessier-Lavigne M (1997) Neuropilin is a receptor for the axonal chemorepellent Semaphorin III. *Cell* 90:739–751.
9. Eickholt BJ, Mackenzie SL, Graham A, Walsh FS, Doherty P (1999) Evidence for collapsin-1 functioning in the control of neural crest migration in both trunk and hindbrain regions. *Development* 126:2181–2189.
10. Kawasaki T, et al. (2002) Requirement of neuropilin 1-mediated Sema3A signals in patterning of the sympathetic nervous system. *Development* 129:671–680.
11. Rao MS, Anderson DJ (1997) Immortalization and controlled in vitro differentiation of murine multipotent neural crest stem cells. *J Neurobiol* 32:722–746.
12. Stern CD, Keynes RJ (1987) Interactions between somite cells: The formation and maintenance of segment boundaries in the chick embryo. *Development* 99:261–272.
13. Serbedzija GN, Bronner-Fraser M, Fraser SE (1992) Vital dye analysis of cranial neural crest cell migration in the mouse embryo. *Development* 116:297–307.
14. Southard-Smith EM, Kos L, Pavan WJ (1998) Sox10 mutation disrupts neural crest development in Dom Hirschsprung mouse model. *Nat Genet* 18:60–64.
15. Vieira JM, Schwarz Q, Ruhrberg C (2007) Selective requirements for neuropilin ligands in neurovascular development. *Development* 134:1833–1843.
16. Kitsukawa T, et al. (1997) Neuropilin-semaphorin III/D-mediated chemorepulsive signals play a crucial role in peripheral nerve projection in mice. *Neuron* 19:995–1005.
17. Gu C, et al. (2003) Neuropilin-1 conveys semaphorin and VEGF signaling during neural and cardiovascular development. *Dev Cell* 5:45–57.
18. Jiang X, Rowitch DH, Soriano P, McMahon AP, Sucov HM (2000) Fate of the mammalian cardiac neural crest. *Development* 127:1607–1616.
19. Taniguchi M, et al. (1997) Disruption of semaphorin III/D gene causes severe abnormality in peripheral nerve projection. *Neuron* 19:519–530.
20. Kubota Y, Morita T, Ito K (1996) New monoclonal antibody (4E9R) identifies mouse neural crest cells. *Dev Dyn* 206:368–378.
21. Kim J, Lo L, Dormand E, Anderson DJ (2003) SOX10 maintains multipotency and inhibits neuronal differentiation of neural crest stem cells. *Neuron* 38:17–31.
22. Lee MK, Tuttle JB, Rebhun LI, Cleveland DW, Frankfurter A (1990) The expression and posttranslational modification of a neuron-specific beta-tubulin isotype during chick embryogenesis. *Cell Motil Cytoskeleton* 17:118–132.
23. Cochard P, Goldstein M, Black IB (1978) Ontogenetic appearance and disappearance of tyrosine hydroxylase and catecholamines in the rat embryo. *Proc Natl Acad Sci USA* 75:2986–2990.
24. Schneider C, Wicht H, Enderich J, Wegner M, Rohrer H (1999) Bone morphogenetic proteins are required in vivo for the generation of sympathetic neurons. *Neuron* 24:861–870.
25. Ericson J, Thor S, Edlund T, Jessell TM, Yamada T (1992) Early stages of motor neuron differentiation revealed by expression of homeobox gene Islet-1. *Science* 256:1555–1560.
26. Eng SR, Lanier J, Fedtsova N, Turner EE (2004) Coordinated regulation of gene expression by Brn3a in developing sensory ganglia. *Development* 131:3859–3870.
27. Kalcheim C, Le Douarin NM (1986) Requirement of a neural tube signal for the differentiation of neural crest cells into dorsal root ganglia. *Dev Biol* 116:451–466.
28. Francis SE, et al. (2002) Central roles of alpha5beta1 integrin and fibronectin in vascular development in mouse embryos and embryoid bodies. *Arterioscler Thromb Vasc Biol* 22:927–933.
29. Newgreen DF, Gibbins IL, Sauter J, Wallenfels B, Wutz R (1982) Ultrastructural and tissue-culture studies on the role of fibronectin, collagen and glycosaminoglycans in the migration of neural crest cells in the fowl embryo. *Cell Tissue Res* 221:521–549.
30. Gammill LS, Gonzalez C, Gu C, Bronner-Fraser M (2006) Guidance of trunk neural crest migration requires neuropilin 2/semaphorin 3F signaling. *Development* 133:99–106.
31. Waimey KE, Huang PH, Chen M, Cheng HJ (2008) Plexin-A3 and plexin-A4 restrict the migration of sympathetic neurons but not their neural crest precursors. *Dev Biol* 315:448–458.
32. Steel KP, Davidson DR, Jackson IJ (1992) TRP-2/DT, a new early melanoblast marker, shows that steel growth factor (c-kit ligand) is a survival factor. *Development* 115:1111–1119.
33. Erickson CA, Goins TL (1995) Avian neural crest cells can migrate in the dorsolateral path only if they are specified as melanocytes. *Development* 121:915–924.
34. Harris ML, Erickson CA (2007) Lineage specification in neural crest cell pathfinding. *Dev Dyn* 236:1–19.
35. Schwarz Q, Vieira JM, Howard B, Eickholt BJ, Ruhrberg C (2008) Neuropilin 1 and 2 control cranial gangliogenesis and axon guidance through neural crest cells. *Development* 135:1605–1613.
36. Riddle RD, Johnson RL, Laufer E, Tabin C (1993) Sonic hedgehog mediates the polarizing activity of the ZPA. *Cell* 75:1401–1416.